Preprints.org

Article

Not peer-reviewed version

Theoretical Study on the Structures and Stabilities of CunZn3O3 (N = 1 – 4) Clusters: Sequential Doping of Zn3O3 Cluster with Cu Atoms

Zhi-Wei Tao , Han-Yi Zou , Hong-Hui Li , Bin Wang * , Wen-Jie Chen *

Posted Date: 27 December 2023

doi: 10.20944/preprints202312.2109.v1

Keywords: Copper-doped zinc oxide clusters; Density functional theory; Structural evolution; Reactivity

Preprints.org is a free multidiscipline platform providing preprint service that is dedicated to making early versions of research outputs permanently available and citable. Preprints posted at Preprints.org appear in Web of Science, Crossref, Google Scholar, Scilit, Europe PMC.

Copyright: This is an open access article distributed under the Creative Commons Attribution License which permits unrestricted use, distribution, and reproduction in any medium, provided the original work is properly cited.

Preprints (www.preprints.org) | NOT PEER-REVIEWED | Posted: 27 December 2023 doi:10.20944/preprints202312.2109.v1

Disclaimer/Publisher's Note: The statements, opinions, and data contained in all publications are solely those of the individual author(s) and contributor(s) and not of MDPI and/or the editor(s). MDPI and/or the editor(s) disclaim responsibility for any injury to people or property resulting from any ideas, methods, instructions, or products referred to in the content.

Article

Theoretical Study on the Structures and Stabilities of $Cu_nZn_3O_3$ (n = 1 - 4) Clusters: Sequential Doping of Zn_3O_3 Cluster with Cu Atoms

Zhi-Wei Tao [1], Han-Yi Zou [1], Hong-Hui Li [1], Bin Wang [1,*] and Wen-Jie Chen [2,*]

[1] College of Chemistry, Fuzhou University, Fuzhou, Fujian, 350108, P. R. China
[2] Department of Material Chemistry, College of Chemical Engineering and Materials, Quanzhou Normal University, Quanzhou, Fujian, 362000, P. R. China
* Correspondence: wangbin_100@fzu.edu.cn (B.W.); chenwenjie@qztc.edu.cn (W.J.C.)

Abstract: Density functional theory (DFT) and coupled cluster theory (CCSD(T)) calculations are performed to investigate the geometric, electronic structures and chemical bonding of a series of Cu-doped zinc oxide clusters, $Cu_nZn_3O_3$ (n = 1-4). The structural evolution of $Cu_nZn_3O_3$ (n = 1-4) clusters are elaborated in our work. The planar seven-membered ring of $CuZn_3O_3$ cluster plays an important role in the structural evolution, that is, the Cu atom, Cu dimer (Cu_2) and Cu trimer (Cu_3) anchor on the $CuZn_3O_3$ cluster. The aggregate behavior of Cu atoms on Zn_3O_3 may offer insight into the study of Cu/ZnO-based catalysts. Additionally, it is found that the $Cu_nZn_3O_3$ clusters become more stable as the Cu content (n) increases. Bader charge analysis points out that as the Cu atoms doping, the reducibility of Cu aggregation (Cu_{n-1}) on the $CuZn_3O_3$ cluster increases. Combined with the d-band centers and the surface electrostatic potential (ESP), the reactivity and the possible reaction sites of $Cu_nZn_3O_3$ (n = 1-4) clusters are also illustrated.

Keywords: copper-doped zinc oxide clusters; density functional theory; structural evolution; reactivity

1. Introduction

Cu-based catalysts have played an important role in industry, such as electrocatalytic reduction of CO_2, methanol steam reforming and water gas shift reaction.[1-4] But at the same time, Cu-based catalysts have still suffered some restrictions, such as thermal instabilities and low selectivity.[1,2] Cu-based catalysts are prone to sintering when the temperature rises above 300 °C.[2] Cu/ZnO catalysts is one of the commonly used Cu-based catalysts, in which Cu usually acts as the main active component, and ZnO plays the dual role of promoter and support.[5] Specifically, Cu^{2+} ions would be reduced to the active Cu^0/Cu^+ species, and the addition of ZnO would increase the copper dispersion and reducibility which are related to the enhanced catalytic activity.[3,6] Meanwhile, the sizes and geometries of the metal nano-particles and the species formed at the Cu-ZnO interface also affect the catalytic properties of Cu/ZnO catalysts. To develop the Cu-based catalysts with superior performance, the precise structures and the structure-activity relationship of catalytic active sites and the interaction of the main active component with the additives including the supports are the fundamental issues that needs to be solved.[7] In this regard, clusters which may serve as the models at the atomic level and the highly active catalytic materials have attracted great research interest.

Recently, well-supported single/dual-atom and cluster catalysts have become the research hotspots.[8-12] Among these, copper oxide clusters have been considered as the catalytic active sites of copper-exchanged zeolites in the methane oxidation to methanol.[12] Herein, copper oxide clusters with the different stoichiometries and sizes were embedded in the channel of zeolites, the geometries, stabilities of these clusters and their underlying correlations with the catalytic activities were elaborated. Additionally, a fully-exposed Cu_7 cluster anchored to the loop-like [6]cycloparaphenylene was found to be highly active and selective in the CO electro-reduction.[11] As for ZnO clusters, it is accepted that $(ZnO)_n$ (n < 8) clusters favored the Zn–O alternating ring

© 2023 by the author(s). Distributed under a Creative Commons CC BY license.

Preprints (www.preprints.org) | NOT PEER-REVIEWED | Posted: 27 December 2023 doi:10.20944/preprints202312.2109.v1

structures. As the size (n) of $(ZnO)_n$ clusters increased to 8, a ring-to-cage transition occurred.[13-15] In these stoichiometric $(ZnO)_n$ (n = 1-13) clusters, $(ZnO)_3$, $(ZnO)_9$ and $(ZnO)_{12}$ were found to possess relatively higher stability.[15] Moreover, the Zn_3O_3 six-membered ring can be found in the larger $(ZnO)_n$ (n > 8) clusters and the hexagonal wurtzite structures of ZnO crystals.[14,16,17] Thus, the relatively stable Zn_3O_3 cluster may be used as a molecular model for the wurtzite ZnO surface.

We have constantly strived to explore the novel chemical bonding and the cluster models to gain further insights into the active sites of complicated catalyst surfaces and the reaction mechanisms of catalytic processes.[18-21] In this work, we make an effort to reveal the evolution rule of the geometric, electronic structures and chemical bonding in the Cu-doped $Cu_nZn_3O_3$ (n = 1-4) clusters. Bader charge analysis, d-band center theory and surface electrostatic potential (ESP) are used to analyze the reactivity and reaction sites of $Cu_nZn_3O_3$ (n = 1-4) clusters. This work may enlighten the aggregation tendency of small Cu clusters on ZnO surface and the structures at the Cu-ZnO interface.

2. Methods

The initial geometries of $Cu_nZn_3O_3$ (n = 1-4) clusters were constructed using the structural searches of the ABCluster program [22,23] in combination with the artificial constructions. These initial geometries were optimized using the B3LYP functional [24-26] in the Gaussian 09 program.[27] The Stuttgart small-core relativistic effective core potential (RECP) was used for the Cu and Zn atoms, whose corresponding basis sets are Cu: [6s,6p,4d,3f,2g], Zn: [6s,6p,4d,3f,2g].[28-31] As for O atoms, the aug-cc-pVTZ basis set was adopted.[32,33] In the structural optimizations, the vibrational frequencies were calculated to ensure that the optimized structures were free of imaginary frequencies. In order to verify the reliability of the above computational methods (denoted as B3LYP/BS), we compared the bond lengths, binding energies, vibrational frequencies and dipole moments of ZnO and CuO molecules from the available experiments with our calculations. As shown in Table S1, our calculations are in agreement with those data from experiments. The low-lying isomers within 0.50 eV at the B3LYP/BS level were then subjected to more accurate coupled cluster CCSD(T) single-point-energy calculations using the Molpro 2010 software.[34] Multiwfn program [35,36] was employed to analyze the Bader charge, surface electrostatic potential (ESP) and d-band centers of $Cu_nZn_3O_3$ (n = 0-4) clusters.

3. Results

It is accepted that Zn_3O_3 cluster is a planar six-membered-ring structure with D_{3h} symmetry (Figure 1a),[13] in which Zn and O atoms are alternately bonded ($d_{Zn\text{-}O}$ = 1.817 Å). The distances between two Zn atoms are 2.654 Å.

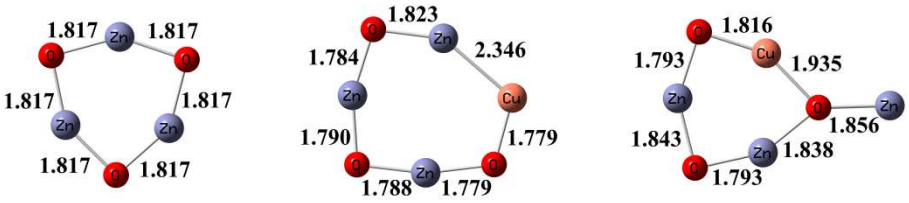

(a) Zn_3O_3 (0.00 D_{3h} $^1A_1'$) (b) $CuZn_3O_3$ (0.00 C_S $^2A'$) (c) $CuZn_3O_3$ (0.50 C_1 ^2A)

Figure 1. Optimized structures ($\Delta E \leq 0.50$ eV) for Zn_3O_3 and $CuZn_3O_3$. The bond lengths are in angstroms and the relative energies (ΔE) in eV are in the parentheses.

3.1. Optimized Structures of $CuZn_3O_3$

$CuZn_3O_3$ clusters are constructed by adding a Cu atom to the most stable Zn_3O_3 cluster. The most stable structure of $CuZn_3O_3$ is shown in Figure 1b, which is consistent with the previous theoretical study.[15] It can be regard as inserting a Cu atom into the Zn-O bond of Zn_3O_3 cluster, leading to the planar seven-membered-ring structure. The second low-lying isomer (Figure 1c) lies 0.50 eV higher in energy, for which the six-membered Zn_3O_3 ring is broken. Other $CuZn_3O_3$ isomers are higher in energy by at least 0.50 eV. They are collected in the Supporting Information (Figure S1).

Preprints (www.preprints.org) | NOT PEER-REVIEWED | Posted: 27 December 2023 doi:10.20944/preprints202312.2109.v1

3.2. Optimized Structures of $Cu_2Zn_3O_3$

To search for the ground state of $Cu_2Zn_3O_3$ cluster, a Cu atom was added to the most stable $CuZn_3O_3$ cluster. The optimized $Cu_2Zn_3O_3$ clusters with the relative energy below 0.50 eV are shown in Figure 2. The ground state of $Cu_2Zn_3O_3$ cluster (Figure 2a) can be viewed as inserting a Cu atom into the Zn-Cu bond of $CuZn_3O_3$ cluster, resulting in a planar eight-membered-ring structure. It is consistent with the earlier finding of $Cu_2Zn_3O_3$ cluster.[15] The Cu-Cu bond length is 2.366 Å, slightly longer than Cu-Zn bond length (2.343 Å). It is in agreement with the covalent radius of the Cu and Zn atoms (d_{Cu} = 1.52 Å, d_{Zn} =1.45 Å)[37] and suggests the metal-metal bonding of the inserting Cu atom with the neighboring Cu and Zn atoms. The second low-lying isomer (Figure 2b) which can be viewed as adding a bridged Cu to the $CuZn_3O_3$ ground state is 0.39 eV less stable than the ground state. Other isomers are found to be much higher in energy (ΔE > 0.50 eV) which are given in the Supporting Information (Figure S2).

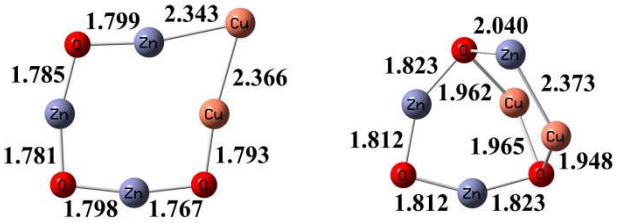

(a) $Cu_2Zn_3O_3$ (0.00 C_S $^1A'$) **(b) $Cu_2Zn_3O_3$ (0.39 C_1 ^1A)**

Figure 2. Optimized structures (ΔE < 0.50 eV) for $Cu_2Zn_3O_3$. The bond lengths are in angstroms and the relative energies (ΔE) in eV are in the parentheses.

3.3. Optimized Structures of $Cu_3Zn_3O_3$

As the number of doped Cu atoms increases, more low-lying isomers appear for the $Cu_3Zn_3O_3$ clusters (Figure 3). The most stable $Cu_3Zn_3O_3$ cluster (Figure 3a) can be seen as adding a copper dimer (Cu_2) between two bridged oxygen atoms of the $CuZn_3O_3$ ground state. At this point, the 3-fold coordinated bridged oxygen atom (μ_3-O) begins to appear in the ground states of $Cu_nZn_3O_3$ clusters. The Cu-Cu bond length of Cu dimer (Cu_2) is 2.388 Å in $Cu_3Zn_3O_3$ cluster which is much longer than that (2.232 Å) of isolated Cu_2 molecule ($D_{\infty h}$ $^1\Sigma_g^+$) at the same calculation level. It is inferred that there are relatively strong interactions of the Cu_2 moiety with the remaining fragment of $Cu_3Zn_3O_3$. As shown in Figure 3, there are several isomers that have energies close to the ground state. To further distinguish the stability of these low-lying isomers, the single-point CCSD(T) calculations were performed using their B3LYP equilibrium geometries. The single-point CCSD(T) calculations still support the structure contained the Cu_2 (Figure 3a) to be the most stable $Cu_3Zn_3O_3$ cluster (Table S2). Other higher-energy isomers (ΔE > 0.50 eV) are shown in the Supporting Information (Figure S3).

Preprints (www.preprints.org) | NOT PEER-REVIEWED | Posted: 27 December 2023 doi:10.20944/preprints202312.2109.v1

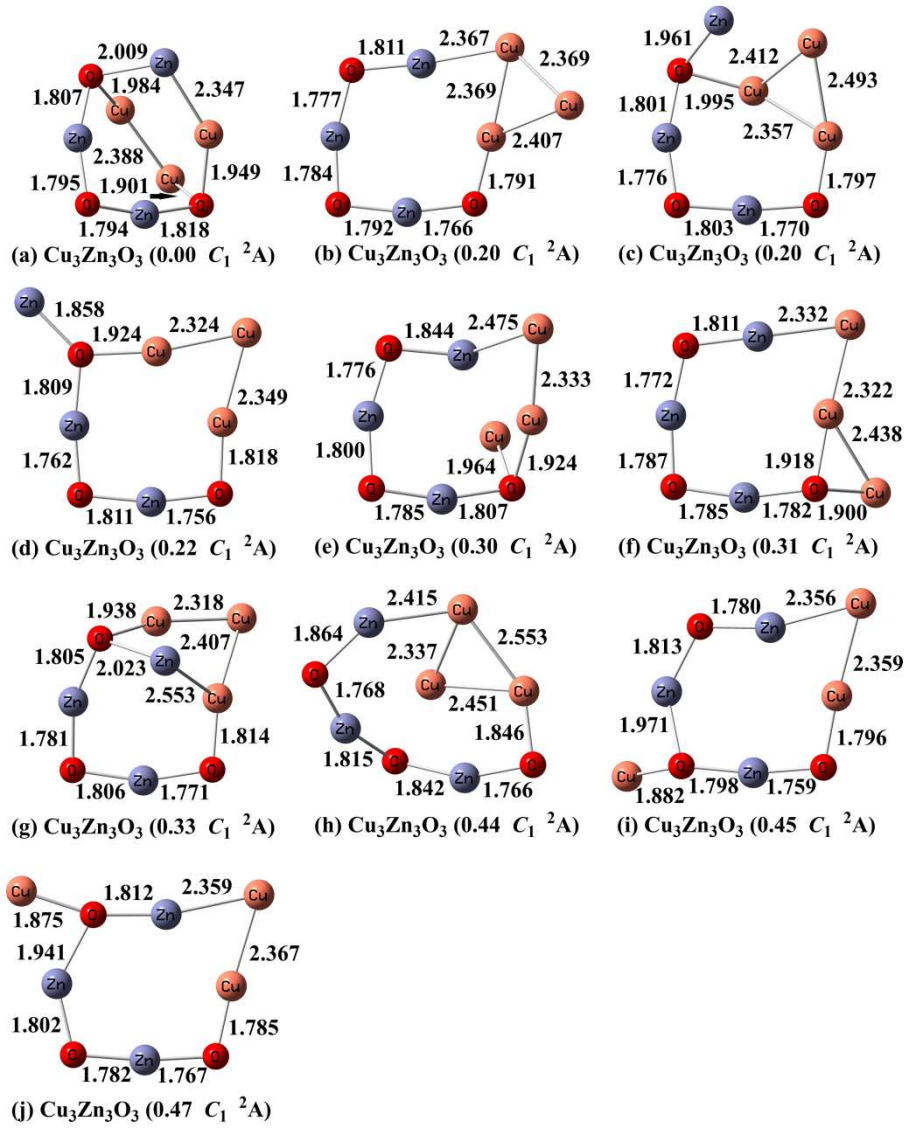

Figure 3. Optimized structures (ΔE < 0.50 eV) for $Cu_3Zn_3O_3$. The bond lengths are in angstroms and the relative energies (ΔE) in eV are in the parentheses.

3.4. Optimized Structures of $Cu_4Zn_3O_3$

In our calculations, the most stable $Cu_4Zn_3O_3$ cluster is shown in Figure 4a. It can be viewed as adding a copper trimer (Cu_3) between two bridged oxygen atoms of the $CuZn_3O_3$ ground state. Meanwhile, several low-lying isomers within 0.50 eV were found (Figure 4). Among them, there is an isomer (Figure 4b) which contains the Cu_4 moiety and is only 0.10 eV higher in energy. The relative energies of these isomers were further refined by the CCSD(T) single-point calculations (Table S2). The CCSD(T) results support the structure shown in Figure 4a to be the most stable one, and the isomer shown in Figure 4b is 0.28 eV less stable. Other higher-energy isomers (ΔE > 0.50 eV) are displayed in the Supporting Information (Figure S4).

Preprints (www.preprints.org) | NOT PEER-REVIEWED | Posted: 27 December 2023 doi:10.20944/preprints202312.2109.v1

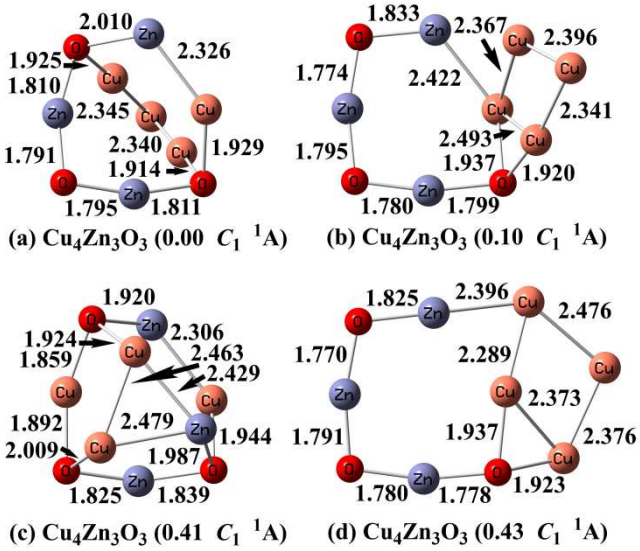

Figure 4. Optimized structures (ΔE < 0.50 eV) for $Cu_2Zn_3O_3$. The bond lengths are in angstroms and the relative energies (ΔE) in eV are in the parentheses.

4. Discussion

4.1. Structural Evolution in $Cu_nZn_3O_3$ (n = 1-4) Clusters and Their Stability

It has been reported that the supported Cu_2 and Cu_3 clusters are the multi-atom cluster catalysts in specific reactions, and appropriate supports could improve their stability and dispersibility.[38,39] Zinc oxides as one of the most common promoter and support for Cu-based catalysts, the Zn_3O_3 six-membered ring is common in the larger $(ZnO)_n$ (n > 8) clusters and the wurtzite ZnO.[14,16,17] Studying the structural evolution of the $Cu_nZn_3O_3$ (n = 1-4) clusters via sequential doping of Zn_3O_3 cluster with Cu atoms may help us gain insight into the aggregation behavior of small Cu clusters on ZnO surface.

For $CuZn_3O_3$, the Cu atom is inserted into the Zn-O bond of Zn_3O_3 cluster. For $Cu_2Zn_3O_3$, the Cu atom is inserted into the Zn-Cu bond of $CuZn_3O_3$ cluster. As for $Cu_3Zn_3O_3$ and $Cu_4Zn_3O_3$ clusters, the planar seven-membered ring of $CuZn_3O_3$ cluster starts to play an important role in the subsequent aggregation of Cu atoms (Figure 5), that is, the Cu dimer (Cu_2) and Cu trimer (Cu_3) are attached to the $CuZn_3O_3$ cluster by two bridged oxygen atom (μ_3-O). Herein, we found that at the low Cu content (n = 1,2), Cu atoms prefer to insert into the Zn-O bond of Zn_3O_3 first, then aggregate to form the $ZnCu_2$ units. The six-membered ring of Zn_3O_3 gradually expanded to the eight-membered ring of $Cu_2Zn_3O_3$. When the Cu content further increases (n = 3,4), the extra Cu atoms aggregate with each other to form Cu_{n-1} units which is supported on $CuZn_3O_3$ cluster.

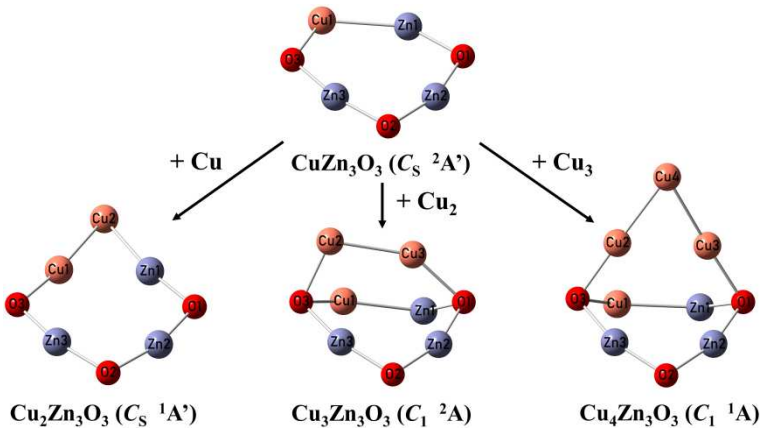

Figure 5. Structural evolution of $Cu_nZn_3O_3$ (n = 1-4) clusters.

Preprints (www.preprints.org) | NOT PEER-REVIEWED | Posted: 27 December 2023 doi:10.20944/preprints202312.2109.v1

The relative stability of $Cu_nZn_3O_3$ (n = 1-4) clusters is evaluated by the calculated atomization energy ($E_{b,1}$). The atomization energy ($E_{b,1}$) of $Cu_nZn_3O_3$ clusters were calculated by the following formula:

$$E_{b,1} = nE(Cu) + 3E(Zn) + 3E(O) - E(Cu_nZn_3O_3) \quad (2)$$

$E(Cu_nZn_3O_3)$, $E(Cu)$, $E(Zn)$ and $E(O)$ represents the energy of $Cu_nZn_3O_3$ ground state, Cu, Zn and O atom, respectively. As seen in Table 1, the $E_{b,1}$ increases gradually with the increase of Cu content. It suggests the $Cu_nZn_3O_3$ clusters become more stable as the Cu atoms doping (n = 0-4).

Table 1. Atomization energy ($E_{b,1}$) of $Cu_nZn_3O_3$ cluster. The energies are in eV.

Cluster	Zn_3O_3	$CuZn_3O_3$	$Cu_2Zn_3O_3$	$Cu_3Zn_3O_3$	$Cu_4Zn_3O_3$
$E_{b,1}$	22.07	24.03	26.68	28.28	31.27

4.2. Chemical Bonding of $Cu_nZn_3O_3$ (n = 1-4) Clusters

It is known that zinc has the electronic configuration of $3d^{10}4s^2$. Usually, its 3d electrons do not participate in bonding with other elements. So in zinc oxides, it almost shows the exclusively +2 oxidation state. But copper as the neighbor element of zinc, it has the $3d^{10}4s^1$ configuration, its 3d electrons participate in the bonding. So the oxidation state of Cu is more abundant (+1, +2 and +3).[40] To better understand the charge transfer in the sequential doping of Zn_3O_3 cluster with Cu atoms, we calculated the Bader charges of the $Cu_nZn_3O_3$ (n = 1-4) clusters (Table 2). For Zn_3O_3 cluster, the Bader charge of Zn and O atom is +1.13 |e| and -1.13 |e|, respectively. Obviously, the oxidation state of Zn and O in Zn_3O_3 cluster is +2 and -2, respectively. Thus, the Bader charge of about ±0.5 |e| is indicative of a single-electron transfer, and the Bader charge of about ±1.0 |e| corresponds to two-electrons transfer.[41]

After inserting a Cu atom into the Zn-O bond of Zn_3O_3 cluster, the Bader charge of the Zn atom (denoted as Zn-1 in Figure 5) next to the newly added Cu atom (denoted as Cu-1) drops to +0.64 |e|, the charge of the Cu-1 atom is +0.43 |e|. In other words, the ZnCu unit in $CuZn_3O_3$ transfers 1.07 |e| to the nearby oxygen atoms (denoted as O-1 and O-3) in total. It is inferred that Zn-1 and Cu-1 atoms each transfer an electron to the adjacent oxygen atoms (O-1 and O-3). It leads to the metal-oxygen single bond. Meanwhile, the remaining 4s electron of Zn-1 forms the metal bond with Cu-1 atom. Continuing adding a Cu atom to the $CuZn_3O_3$ cluster, the added Cu atom (denoted as Cu-2) inserts into the Zn-Cu bond of $CuZn_3O_3$ cluster. As given in Table 2, the Bader charge of Cu-2 is approximately zero (+0.02 |e|). It could be understood by the formation of metal bonds between the Cu-2 atom and the Zn-1 and Cu-1 atoms. Herein, $ZnCu_2$ unit in $Cu_2Zn_3O_3$ cluster transfers 1.14 |e| to the adjacent oxygen atoms (O-1 and O-3) in total. Compared with Zn_3O_3 cluster, the charges on the other atoms do not change much.

For $Cu_nZn_3O_3$ (n = 3,4) clusters, they can be viewed as adding the Cu_2 (Cu-2 and Cu-3) and Cu_3 (Cu-2, Cu-3 and Cu-4) to the $CuZn_3O_3$ cluster linked by two 3-fold coordinated oxygen atoms (O-1 and O-3). Compared with the ZnCu diatom of $CuZn_3O_3$ cluster, the Bader charge of Zn-1 reduces from +0.64 |e| to +0.37 |e|, and the charge of Cu-1 also decreases from +0.43 |e| to roughly +0.3 |e|. It suggested less charge transfers from the ZnCu diatom of $Cu_nZn_3O_3$ (n = 3,4) to the O-1 and O-3 atoms. As compensation, the newly added Cu_2 and Cu_3 units in $Cu_nZn_3O_3$ (n = 3,4) transfer charges of +0.51 |e| and +0.56 |e| to the O-1 and O-3 atoms. To analyze the interaction of Cu aggregation (Cu_{n-1}) with $CuZn_3O_3$ cluster, the binding energies ($E_{b,2}$) of the isolated Cu_{n-1} clusters with $CuZn_3O_3$ cluster were calculated by the following formula:

$$E_{b,2} = E(Cu_nZn_3O_3) - E(CuZn_3O_3) - E(Cu_{n-1}) \quad (1)$$

Preprints (www.preprints.org) | NOT PEER-REVIEWED | Posted: 27 December 2023 doi:10.20944/preprints202312.2109.v1

$E(Cu_nZn_3O_3)$, $E(CuZn_3O_3)$ and $E(Cu_{n-1})$ represents the ground-state energy of $Cu_nZn_3O_3$, $CuZn_3O_3$ and Cu_{n-1} clusters, respectively. The $E_{b,2}$ of Cu_2 in $Cu_3Zn_3O_3$ cluster is calculated to be -1.60 eV, and that of Cu_3 in $Cu_4Zn_3O_3$ cluster is -3.21 eV. The more negative $E_{b,2}$ means the stronger interaction between Cu aggregation (Cu_{n-1}) and $CuZn_3O_3$ cluster, and higher stability of Cu_{n-1} on the $CuZn_3O_3$ seven-membered ring. Here, the more negative binding energies ($E_{b,2}$) coincides with the more transferred charge from Cu_{n-1} to $CuZn_3O_3$. For Cu/ZnO catalysts, the addition of ZnO is conducive to increasing the dispersion and reducibility of the active copper component.[42] From the perspective of Bader charge, the Cu_{n-1} in $Cu_nZn_3O_3$ (n = 3,4) is more reducible than the Cu_n in $Cu_nZn_3O_3$ (n = 1,2). The synergistic interaction between Cu and Zn in $CuZn_3O_3$ may enhance the reducibility of Cu species in $Cu_nZn_3O_3$ (n = 3,4).

Table 2. Bader charges (|e|) analysis of $Cu_nZn_3O_3$ (n = 0-4).

Cluster	Zn-1	Zn-2	Zn-3	O-1	O-2	O-3	Cu-1	Cu-2	Cu-3	Cu-4
Zn_3O_3	1.13	1.13	1.13	-1.13	-1.13	-1.13				
$CuZn_3O_3$	0.64	1.12	1.15	-1.15	-1.14	-1.06	0.43			
$Cu_2Zn_3O_3$	0.75	1.14	1.12	-1.15	-1.15	-1.10	0.37	0.02		
$Cu_3Zn_3O_3$	0.37	1.11	1.12	-1.16	-1.14	-1.09	0.28	0.25	0.26	
$Cu_4Zn_3O_3$	0.37	1.12	1.11	-1.17	-1.14	-1.11	0.26	0.31	0.31	-0.06

4.3. Reactivity of $Cu_nZn_3O_3$ (n = 1-4) Clusters

The model of d-band center was developed by Nørskov and co-workers[43] and was used as an important descriptor to determine the reactivity of surfaces and clusters.[44-48] The partial density of states (PDOS) for the d-orbitals of metal atoms in $Cu_nZn_3O_3$ (n = 0-4) clusters are depicted in Figure 6, and the d-band centers (ε_d) are denoted by the red solid line. For the open-shell systems, the spin up (α) and spin down (β) d-band centers (ε_d) were calculated separately (Table S3), and the spin down ones were always higher in energy. So we uniformly use the spin down d-band centers (ε_d) for the subsequent comparison. The energy level of highest occupied molecular orbital (HOMO-β) are marked by the blue dashed line. For comparison, all HOMO energy levels in Figure 6 are shifted to zero. As shown in Figure 6f, the ε_d move toward HOMO-β as the Cu content (n) increases. It suggests the interaction between nucleophilic molecules and the metal atoms become stronger as the Cu content (n) increases.[44,47] It also infers the reactivity of $Cu_nZn_3O_3$ (n = 0-4) clusters increase as the Cu content (n) increases.

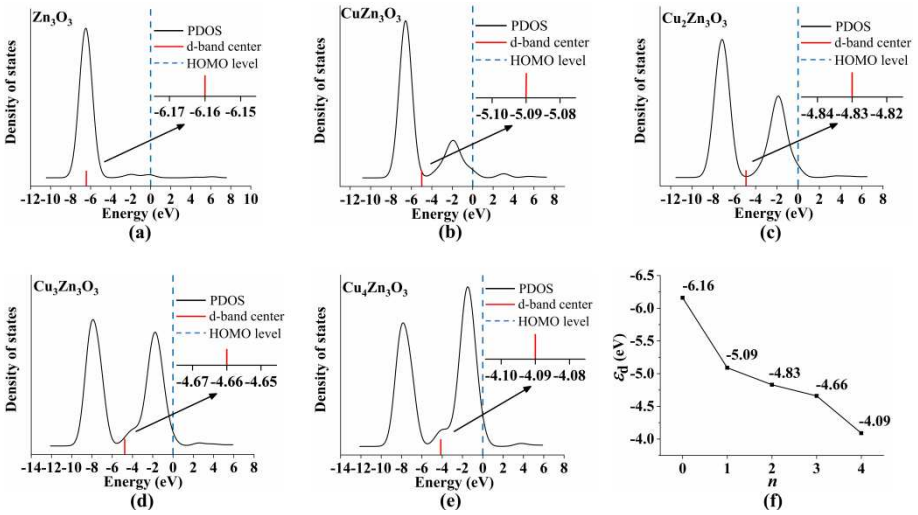

Figure 6. (a)-(e) The d-band density of states for the lowest-energy $Cu_nZn_3O_3$ (n = 0-4) clusters. The inset is the enlarged drawing of the d-band center. (f) The d-band center (ε_d) as a function of Cu content (n) in $Cu_nZn_3O_3$ (n = 0-4) clusters.

Preprints (www.preprints.org) | NOT PEER-REVIEWED | Posted: 27 December 2023 doi:10.20944/preprints202312.2109.v1

The electrostatic potential (ESP) provides a way of identifying the active sites.[44,49] The surface ESP for $Cu_nZn_3O_3$ (n = 1-4) clusters are shown in Figure 7. Obviously, the red-colored (positive ESP) regions are positioned at the metal atoms, and the ESP of $Cu_nZn_3O_3$ clusters are less localized compared with the Zn_3O_3 clusters. Additionally, the cyan and yellow tiny spheres in Figure 7 point out the locations of the extreme points of the surface ESP, and the arrows indicate the extreme points with the maximum absolute values. The sites with the most positive values of molecular ESP are associated with the ideal adsorption positions for nucleophilic reagents, whereas the most negative ESP are related to that of electrophilic reagents. In this series of $Cu_nZn_3O_3$ (n = 1-4) clusters, the most positive regions of ESP are always nearby the Zn-2 atom except for $Cu_2Zn_3O_3$. Except for $Cu_2Zn_3O_3$, the other $Cu_nZn_3O_3$ clusters can be viewed as adding the Cu_2 and Cu_3 units to the $CuZn_3O_3$ cluster linked by two 3-fold coordinated oxygen atoms (O-1 and O-3). For $Cu_2Zn_3O_3$, the newly added Cu atom (Cu-2) expands the seven-membered ring of $CuZn_3O_3$ to the eight-membered ring. The most positive region of ESP of $Cu_2Zn_3O_3$ is nearby the newly added Cu-2 atom. In $Cu_nZn_3O_3$ (n = 1-4) clusters, the ESP of 3-fold coordinated oxygen atoms are more negative than that of 2-fold coordinated oxygen atoms. For $CuZn_3O_3$ and $Cu_2Zn_3O_3$, the most negative regions are located near the O-1 or O-3 atom. For $Cu_3Zn_3O_3$ and $Cu_4Zn_3O_3$, the most negative regions are located near the O-2 atoms. They infer the sensitivity of reactivity to the structures.

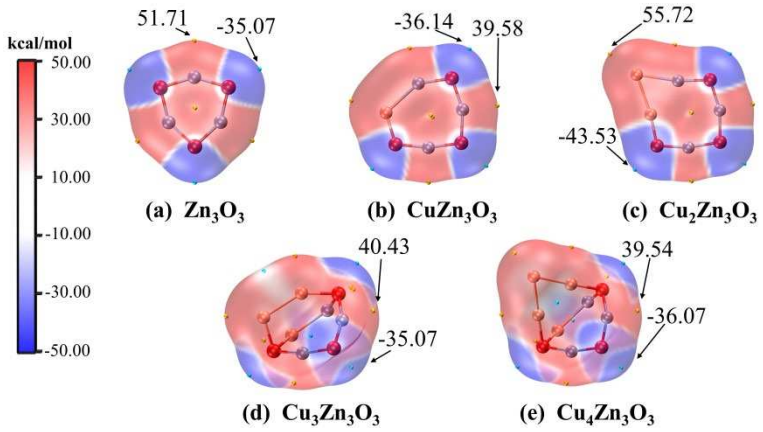

Figure 7. The electrostatic potential (ESP) map on the van der Waals surface for the lowest-energy $Cu_nZn_3O_3$ (n = 0-4) clusters.

5. Conclusions

We report a systematic theoretical study of a series of copper-doped zinc oxide clusters: $Cu_nZn_3O_3$ (n = 1-4). The geometric, electronic structures and chemical bonding of $Cu_nZn_3O_3$ (n = 1-4) clusters are investigated by extensive density functional theory (DFT) and coupled cluster theory (CCSD(T)) calculations. The structural evolutions of $Cu_nZn_3O_3$ (n = 1-4) clusters are found in our work. At the low Cu content (n = 1,2), Cu atoms prefer to insert into the Zn-O bond of Zn_3O_3 first, then aggregate to form the $ZnCu_2$ units. The six-membered ring of Zn_3O_3 gradually expands to the eight-membered ring of $Cu_2Zn_3O_3$. When the Cu content further increases (n = 3,4), the extra Cu atoms aggregate with each other to form Cu_{n-1} units on the $CuZn_3O_3$ cluster. Additionally, relative stability of $Cu_nZn_3O_3$ (n = 1-4) clusters is evaluated. The $Cu_nZn_3O_3$ clusters become more stable as the Cu atoms doping (n = 1-4). Bader charge analysis suggests that as the Cu content (n) increases, the reducibility of Cu aggregation (Cu_{n-1}) on the $CuZn_3O_3$ cluster increase. The studies on d-band centers of $Cu_nZn_3O_3$ (n = 0-4) clusters infer the reactivity also increase as the Cu content (n) increases. The information on the possible reaction site of $Cu_nZn_3O_3$ (n = 1-4) clusters are predicted by the surface electrostatic potential (ESP) calculations.

Supplementary Materials: he following supporting information can be downloaded at the website of this paper posted on Preprints.org. Table S1: Calculated results at the B3LYP/BS level for the bond lengths, binding energies and other properties of ZnO and CuO along with the corresponding available experimental data. Table S2: Relative energies of $Cu_nZn_3O_3$ (n = 1-4) clusters which were further refined by the CCSD(T) single-point

Preprints (www.preprints.org) | NOT PEER-REVIEWED | Posted: 27 December 2023 doi:10.20944/preprints202312.2109.v1

calculations. Table S3: The calculated d-band centers for the spin up (α), spin down (β) and both spin modes of $Cu_nZn_3O_3$ (n = 0-4) clusters. Figures S1-S4: Alternative optimized structures for $Cu_nZn_3O_3$ (n = 1-4) clusters at the B3LYP/BS level. Table S4: Cartesian coordinates for the optimized $Cu_nZn_3O_3$ (n = 0-4) clusters.

Author Contributions: Investigation, Z.W.T.; visualization, H.Y.Z. and H.H.L.; writing—original draft preparation, Z.W.T. and H.Y.Z.; writing—review and editing, B.W. and W.J.C. All authors have read and agreed to the published version of the manuscript.

Funding: This work was supported by the National Natural Science Foundation of China (21301030 and 21603117).

Data Availability Statement: The data presented in this study are available from the corresponding authors upon reasonable request.

Acknowledgments: The authors gratefully acknowledge supports from the National Natural Science Foundation of China (21301030and 21603117).

Conflicts of Interest: The authors declare no conflict of interest.

References

1. Xiao, C.; Zhang, J. Architectural Design for Enhanced C_2 Product Selectivity in Electrochemical CO_2 Reduction Using Cu-Based Catalysts: A Review. *ACS Nano* **2021**, *15*, 7975-8000, doi:10.1021/acsnano.0c10697.
2. Ye, R.; Xiao, S.; Lai, Q.; Wang, D.; Huang, Y.; Feng, G.; Zhang, R.; Wang, T. Advances in Enhancing the Stability of Cu-Based Catalysts for Methanol Reforming. *Catalysts* **2022**, *12*, 747, doi:10.3390/catal12070747.
3. Saw, S.K.; Datta, S.; Chavan, P.D.; Gupta, P.K.; Kumari, S.; Sahu, G.; Chauhan, V. Significance and influence of various promoters on Cu-based catalyst for synthesizing methanol from syngas: a critical review. *Journal of Chemical Technology And Biotechnology* **2023**, *98*, 1083-1102, doi:10.1002/jctb.7331.
4. Teng, M.; Ye, J.; Wan, C.; He, G.; Chen, H. Research Progress on Cu-Based Catalysts for Electrochemical Nitrate Reduction Reaction to Ammonia. *Industrial & Engineering Chemistry Research* **2022**, *61*, 14731−14746, doi:10.1021/acs.iecr.2c02495.
5. Hou, R.; Qiu, R.; Sun, K. Progress in the Cu-based catalyst supports for methanol synthesis from CO_2. *Chemical Industry and Engineering Progress* **2020**, *39*, 2639-2647.
6. Velu, S.; Suzuki, K. Selective Production of Hydrogen for Fuel Cells Via Oxidative Steam Reforming of Methanol Over CuZnAl Oxide Catalysts: Effect of Substitution of Zirconium and Cerium on the Catalytic Performance. *Topics in Catalysis* **2003**, *22*, 235-244, doi:10.1023/A:1023576020120.
7. Ranjekar, A.M.; Yadav, G.D. Steam Reforming of Methanol for Hydrogen Production: A Critical Analysis of Catalysis, Processes, and Scope. *Industrial & Engineering Chemistry Research* **2021**, *60*, 89-113, doi:10.1021/acs.iecr.0c05041.
8. Hou, C.-C.; Wang, H.-F.; Li, C.; Xu, Q. From metal–organic frameworks to single/dual-atom and cluster metal catalysts for energy applications. *Energy Environ. Sci.* **2020**, *13*, 1658-1693, doi:10.1039/C9EE04040D.
9. Qiao, B.; Wang, A.; Yang, X.; Allard, L.F.; Jiang, Z.; Cui, Y.; Liu, J.; Li, J.; Zhang, T. Single-atom catalysis of CO oxidation using Pt_1/FeO_x. *Nature Chemistry* **2011**, *3*, 634-641, doi:10.1038/nchem.1095.
10. Qin, R.; Liu, P.; Fu, G.; Zheng, N. Strategies for Stabilizing Atomically Dispersed Metal Catalysts. *Small Methods* **2018**, *2*, 1700286, doi:10.1002/smtd.201700286.
11. Liu, Y.-Q.; Qiu, Z.-Y.; Zhao, X.; Wang, W.-W.; Dang, J.-S. Trapped copper in [6]cycloparaphenylene: a fully-exposed Cu_7 single cluster for highly active and selective CO electro-reduction. *Journal of Materials Chemistry A* **2021**, *9*, 25922-25926, doi:10.1039/D1TA06688A.
12. Palagin, D.; Knorpp, A.J.; Pinar, A.B.; Ranocchiari, M.; van Bokhoven, J.A. Assessing the relative stability of copper oxide clusters as active sites of a CuMOR zeolite for methane to methanol conversion: size matters? *Nanoscale* **2017**, *9*, 1144-1153, doi:10.1039/C6NR07723D.
13. Matxain, J.M.; Fowler, J.E.; Ugalde, J.M. Small clusters of II-VI materials: Zn_iO_i , i=1 –9. *Physical Review A* **2000**, *62*, 053201, doi:10.1103/PhysRevA.62.053201.
14. Fernando, A.; Dimuthu, K.L.; Weerawardene, M.; Karimova, N.V.; Aikens, C.M. Quantum Mechanical Studies of Large Metal, Metal Oxide, and Metal Chalcogenide Nanoparticles and Clusters. *Chemical Reviews* **2015**, *115*, 6112-6216, doi:10.1021/cr500506r.
15. Yong, Y.; Wang, Z.; Liu, K.; Song, B.; He, P. Structures, stabilities, and magnetic properties of Cu-doped Zn_nO_n (n=3,9,12) clusters: A theoretical study. *Computational and Theoretical Chemistry* **2012**, *989*, 90-96, doi:10.1016/j.comptc.2012.03.011.
16. Tayade, N.T.; Mane, S.M.; Shende, A.T.; Tirpude, M.P.; Shin, J.C. Dissociation of ZnO ring from Zn_3O_3 cluster by CASSCF. *Chemical Physics* **2021**, *542*, 111077, doi:10.1016/j.chemphys.2020.111077.

Preprints (www.preprints.org) | NOT PEER-REVIEWED | Posted: 27 December 2023 doi:10.20944/preprints202312.2109.v1

17. Jin, W.; Chen, G.; Duan, X.; Yin, Y.; Ye, H.; Wang, D.; Yu, J.; Mei, X.; Wu, Y. Adsorption behavior of formaldehyde on ZnO (101¯0) surface: A first principles study. *Applied Surface Science* **2017**, *423*, 451-456, doi:10.1016/j.apsusc.2017.06.125.
18. Wang, B.; Xia, C.-J.; Fang, H.-L.; Chen, W.-J.; Zhang, Y.-F.; Huang, X. Mononuclear thorium halide clusters ThX_4 (X = F, Cl): gas-phase hydrolysis reactions. *Physical Chemistry Chemical Physics* **2018**, *20*, 21184-21193, doi:10.1039/c8cp03071e.
19. Wang, B.; Xie, L.; Liu, X.-J.; Chen, W.-J.; Zhang, Y.-F.; Huang, X. Structural Evolution and Chemical Bonding of Di-Niobium Boride Clusters $Nb_2B_x^{-/0}$ (x = 1-6): Hexagonal Bipyramid $Nb_2B_6^{-/0}$ Species. *European Journal Of Inorganic Chemistry* **2018**, *2018*, 940-950, doi:10.1002/ejic.201701278.
20. Wang, B.; Zhang, S.-Y.; Ye, L.-H.; Zhang, X.-F.; Zhang, Y.-F.; Chen, W.-J. Exploring the Reaction Mechanism of H_2S Decomposition with MS_3 (M = Mo, W) Clusters. *ACS Omega* **2020**, *5*, 13324-13332, doi:10.1021/acsomega.0c01430.
21. Wang, B.; Wu, N.; Zhang, X.-B.; Huang, X.; Zhang, Y.-F.; Chen, W.-K.; Ding, K.-N. Probing the Smallest Molecular Model of MoS_2 Catalyst: S_2 Units in the $MoS_n^{-/0}$ (n= 1–5) Clusters. *Journal of Physical Chemistry A* **2013**, *117*, 5632-5641, doi:10.1021/jp309163c.
22. Zhang, J.; Dolg, M. ABCluster: the artificial bee colony algorithm for cluster global optimization. *Physical Chemistry Chemical Physics* **2015**, *17*, 24173-24181, doi:10.1039/C5CP04060D.
23. Zhang, J.; Dolg, M. Global optimization of clusters of rigid molecules using the artificial bee colony algorithm. *Physical Chemistry Chemical Physics* **2016**, *18*, 3003-3010, doi:10.1039/C5CP06313B.
24. Becke, A.D. A new mixing of Hartree-Fock and local density-functional theories. *Journal of Chemical Physics* **1993**, *98*, 1372-1377, doi:10.1063/1.464304.
25. Lee, C.; Yang, W.; Parr, R.G. Development of the Colle-Salvetti correlation-energy formula into a functional of the electron density. *Physical Review B* **1988**, *37*, 785-789, doi:10.1103/PhysRevB.37.785.
26. Stephens, P.J.; Devlin, F.J.; Chabalowski, C.F.; Frisch, M.J. Ab Initio Calculation of Vibrational Absorption and Circular Dichroism Spectra Using Density Functional Force Fields. *Journal of Physical Chemistry* **1994**, *98*, 11623-11627, doi:10.1021/j100046a014.
27. Frisch, M.J.; Trucks, G.W.; Schlegel, H.B.; Scuseria, G.E.; Robb, M.A.; Cheeseman, J.R.; Scalmani, G.; Barone, V.; Mennucci, B.; Petersson, G.A.; et al. Gaussian 09, Revision C.01. *Gaussian, Inc., Wallingford CT* **2010**.
28. Andrae, D.; Häußermann, U.; Dolg, M.; Stoll, H.; Preuß, H. Energy-adjusted ab initio pseudopotentials for the second and third row transition elements. *Theoretica Chimica Acta* **1990**, *77*, 123-141. ECP parameters for Mo and W were obtained from the following web-site: https://www.basissetexchange.org/, doi:10.1007/BF01114537.
29. Küchle, W.; Dolg, M.; Stoll, H.; Preuss, H. Energy-adjusted pseudopotentials for the actinides. Parameter sets and test calculations for thorium and thorium monoxide. *Journal of Chemical Physics* **1994**, *100*, 7535-7542, doi:10.1063/1.466847.
30. Cao, X.; Dolg, M. Segmented contraction scheme for small-core actinide pseudopotential basis sets. *Journal of Molecular Structure (THEOCHEM)* **2004**, *673*, 203-209, doi:10.1016/j.theochem.2003.12.015.
31. Cao, X.; Dolg, M.; Stoll, H. Valence basis sets for relativistic energy-consistent small-core actinide pseudopotentials. *Journal of Chemical Physics* **2003**, *118*, 487-496, doi:10.1063/1.1521431.
32. Kendall, R.A.; Dunning Jr., T.H.; Harrison, R.J. Electron affinities of the first-row atoms revisited. Systematic basis sets and wave functions. *Journal of Chemical Physics* **1992**, *96*, 6796-6806, doi:10.1063/1.462569.
33. Dunning Jr., T.H. Gaussian basis sets for use in correlated molecular calculations. I. The atoms boron through neon and hydrogen. *Journal of Chemical Physics* **1989**, *90*, 1007-1023, doi:10.1063/1.456153.
34. Werner, H.J.; Knowles, P.J.; Manby, F.R.; Schütz, M.; Celani, P.; Knizia, G.; Korona, T.; Lindh, R.; Mitrushenkov, A.; Rauhut, G.; et al. *MOLPRO, version 2010.1, a package of ab initio programs; see http://www.molpro.net.*
35. Lu, T.; Chen, F. Multiwfn: A multifunctional wavefunction analyzer. *Journal of Computational Chemistry* **2012**, *33*, 580-592, doi:10.1002/jcc.22885.
36. Zhang, J.; Lu, T. Efficient evaluation of electrostatic potential with computerized optimized code. *Physical Chemistry Chemical Physics* **2021**, *23*, 20323-20328, doi:10.1039/D1CP02805G.
37. Lide, D.R. *CRC Handbook of Chemistry and Physics, 89th edition*; CRC Press/Taylor and Francis: Boca Raton, Florida, 2008.
38. Chen, Z.W.; Yan, J.M.; Zheng, W.T.; Jiang, Q. Cu_4 Cluster Doped Monolayer MoS_2 for CO Oxidation. *Scientific Reports* **2015**, *5*, 11230, doi:10.1038/srep11230.
39. Chen, Z.W.; Chen, L.X.; Yang, C.C.; Jiang, Q. Atomic (single, double, and triple atoms) catalysis: frontiers, opportunities, and challenges. *Journal of Materials Chemistry A* **2019**, *7*, 3492-3515, doi:10.1039/C8TA11416A.
40. Nicholls, D. Copper. In *Complexes and First-Row Transition Elements*; Macmillan Education UK: London, 1974; pp. 201-206.
41. Thang, H.V.; Pacchioni, G. Spontaneous Formation of Gold Cluster Anions on ZnO/Cu(111) Bilayer Films. *The Journal of Physical Chemistry C* **2019**, *123*, 7644-7653, doi:10.1021/acs.jpcc.8b03479.

Preprints (www.preprints.org) | NOT PEER-REVIEWED | Posted: 27 December 2023 doi:10.20944/preprints202312.2109.v1

42. Fierro, G.; Lo Jacono, M.; Inversi, M.; Porta, P.; Cioci, F.; Lavecchia, R. Study of the reducibility of copper in CuO-ZnO catalysts by temperature-programmed reduction. *Applied Catalysis A: General* **1996**, *137*, 327-348, doi:10.1016/0926-860X(95)00311-8.
43. Hammer, B.; Nørskov, J.K. Electronic factors determining the reactivity of metal surfaces. *Surface Science* **1995**, *343*, 211-220, doi:10.1016/0039-6028(96)80007-0.
44. Rodríguez-Kessler, P.L.; Rodríguez-Domínguez, A.R.; Muñoz-Castro, A. On the structure and reactivity of Pt_nCu_n (n = 1–7) alloy clusters. *Physical Chemistry Chemical Physics* **2021**, *23*, 7233-7239, doi:10.1039/D1CP00379H.
45. Gao, G.; Waclawik, E.R.; Du, A. Computational screening of two-dimensional coordination polymers as efficient catalysts for oxygen evolution and reduction reaction. *Journal of Catalysis* **2017**, *352*, 579-585, doi:10.1016/j.jcat.2017.06.032.
46. Takagi, N.; Ishimura, K.; Fukuda, R.; Ehara, M.; Sakaki, S. Reaction Behavior of the NO Molecule on the Surface of an M_n Particle (M = Ru, Rh, Pd, and Ag; n = 13 and 55): Theoretical Study of Its Dependence on Transition-Metal Element. *The Journal of Physical Chemistry A* **2019**, *123*, 7021-7033, doi:10.1021/acs.jpca.9b04069.
47. Zhang, Q.; Guo, L. Mechanism of the Reverse Water–Gas Shift Reaction Catalyzed by Cu_{12}TM Bimetallic Nanocluster: A Density Functional Theory Study. *Journal of Cluster Science* **2018**, *29*, 867-877, doi:10.1007/s10876-018-1346-x.
48. Megha; Mondal, K.; Ghanty, T.K.; Banerjee, A. Adsorption and Activation of CO_2 on Small-Sized Cu–Zr Bimetallic Clusters. *The Journal of Physical Chemistry A* **2021**, *125*, 2558-2572, doi:10.1021/acs.jpca.1c00751.
49. Arteca, G.A.; Hernández-Laguna, A.; Rández, J.J.; Smeyers, Y.G.; Mezey, P.G. A topological analysis of molecular electrostatic potential on van der Waals surfaces for histamine and 4-substituted derivatives as H_2-receptor agonists. *Journal of Computational Chemistry* **1991**, *12*, 705-716, doi:10.1002/jcc.540120608.

Disclaimer/Publisher's Note: The statements, opinions and data contained in all publications are solely those of the individual author(s) and contributor(s) and not of MDPI and/or the editor(s). MDPI and/or the editor(s) disclaim responsibility for any injury to people or property resulting from any ideas, methods, instructions or products referred to in the content.